

# Spatial Frequency Combs and Supercontinuum Generation in One-Dimensional Photonic Lattices

Rong Dong, Christian E. Rüter, and Detlef Kip

*Institute of Physics and Physical Technologies, Clausthal University of Technology, 38678 Clausthal-Zellerfeld, Germany*

Ofer Manela and Mordechai Segev

*Department of Physics, Solid State Institute, Technion, Haifa 32000, Israel*

Chengliang Yang and Jingjun Xu

*Key Laboratory of Weak-Light Nonlinear Photonics, Nankai University, Tianjin 300457, People's Republic of China*  
(Received 4 June 2008; revised manuscript received 25 August 2008; published 30 October 2008)

We experimentally demonstrate the formation of spatial supercontinuum and of spatial frequency combs in nonlinear photonic lattices. This process results from multiple four-wave mixing initiated by launching two Floquet-Bloch modes into a one-dimensional lattice. The dynamics of the waves is sensitively dependent on the transverse momentum difference between the two initial modes: when this momentum difference is commensurable with the lattice momentum the waves evolve into a frequency comb, whereas when it is incommensurable the waves evolve into a supercontinuum of spatial frequencies.

DOI: 10.1103/PhysRevLett.101.183903

PACS numbers: 42.25.Fx, 42.65.Tg, 42.65.Wi, 42.82.Et

The past few decades have witnessed growing interest in wave propagation in nonlinear media having a periodically modulated potential [1], starting with the pioneering work of Fermi, Pasta, and Ulam on wave motion in periodic particle-chains with nonlinear coupling [2]. The interplay between nonlinearity and transport properties in a periodic structure enables nonlinear lattices to exhibit intriguing properties such as lattice modulation instability [3–5], lattice solitons [5–7], and interactions among such solitons [8,9] and among Bloch waves [10], all having no analogue in homogeneous media. Specifically in the optical domain, arrays of evanescently coupled channel waveguides are a prominent example of such nonlinear lattices. These arrays consist of equally spaced identical waveguide elements, displaying all inherent properties of a photonic crystal structure, such as Brillouin zones (BZ), forbidden and allowed bands, and so on. Nonlinear waveguide arrays were realized in different materials including semiconductors [11–13], quadratic media [14], photorefractive crystals [15,16], liquid crystals [17], etc. They provide an excellent platform where nonlinear wave propagation can be directly observed and investigated experimentally [3–17].

In another domain of nonlinear waves in periodic structures-photonic crystal fibers (PCFs)-another effect was demonstrated experimentally in 1999: supercontinuum (SC) generation [18], which describes the evolution of a relatively narrow-band ultrashort optical pulse into a broad continuous spectrum [18], typically spanning an optical octave or more. This phenomenon results from the collective action of the whole set of nonlinear optical effects, such as four-wave mixing (FWM), self- and cross-phase modulation, and stimulated Raman scattering, often accompanied by soliton formation as well as modulation

instability [19,20]. The SC generation phenomenon was actually first observed in 1970 [21] in bulk glass. The unusual chromatic dispersion characteristics of PCFs [22] facilitate a strong nonlinear interaction over a significant length of the fiber.

Unlike the extensive studies on temporal SC in PCFs, the dynamics of spatial SC remained unexplored until recently, when the idea of generating spatial SC and frequency combs (FC) in nonlinear photonic lattices were proposed [23]. The process starts with two Floquet-Bloch (FB) modes [with quasimomenta (QM)  $k_{x1,2}$ ] which interact with one another via FWM. The interaction couples power to new FB modes, spreading to more and more modes which are evenly spaced in momentum space. After sufficiently long propagation distances, the power distribution among the FB modes becomes a comb or a SC structure, depending sensitively on whether or not the momentum difference between the two initial modes is commensurable (or not) to the lattice momentum. This dynamics applies to both focusing and defocusing nonlinearities. Here we demonstrate these effects experimentally: the generation of spatial SC and of spatial FC in nonlinear photonic lattices.

Consider a one-dimensional (1D) nonlinear waveguide array, which is periodically modulated in the transverse direction  $x$ , but is invariant along the propagation direction  $z$ . When the nonlinear action is not too large, the linear FB modes still form a base for describing wave propagation in the lattice; however they couple power to one another (coupled-mode regime). Following Bloch's theorem, the superposition of FB modes (for simplicity, we restrict the sum to the first band) can be written as  $\sum_k A_k(z)U_k(x) \times \exp(i\beta_k z)$ , where  $k$  is the QM and  $\beta_k$  is the propagation

constant of the mode. Here  $U_k(x) = u_k(x) \exp(ikx)$ , and  $u_k(x + \Lambda) = u_k(x)$  are periodic functions with (lattice) period  $\Lambda$ . By solving the nonlinear Schrödinger equation, the coupled-mode equations for the amplitudes  $A_k(z)$  are obtained [23]:

$$i \frac{dA_{k_4}}{dz} \pm \sum_{k_1 k_2 k_3} C_{k_1 k_2 k_3 k_4} A_{k_1}(z) A_{k_2}(z) A_{k_3}^*(z) \exp(i\Delta\beta z) = 0. \quad (1)$$

Here  $\Delta\beta = \beta_1 + \beta_2 - \beta_3 - \beta_4$  is the longitudinal phase mismatch, and the plus/minus sign corresponds to the sign of the nonlinearity. Because of the symmetry properties of FB modes, the tensor  $C_{k_1 k_2 k_3 k_4}$  can be described as

$$C_{k_1 k_2 k_3 k_4} = N \int_0^\Lambda u_{k_1}(x) u_{k_2}(x) u_{k_3}^*(x) u_{k_4}^*(x) \exp(i\Delta k x) dx. \quad (2)$$

Here  $N$  is the number of lattice sites,  $G = 2\pi/\Lambda$  is the lattice momentum (width of the BZ), and  $\Delta k = k_{x1} + k_{x2} - k_{x3} - k_{x4} = nG$  (with  $n = 0, 1, 2, \dots$ ,  $C_{k_1 k_2 k_3 k_4} = 0$  when  $\Delta k$  does not satisfy this relation). When the two FB modes are initially excited at  $z = 0$ , and assuming a sufficient long distance of propagation, a cascaded excitation of modes is triggered. Modes with QM  $k_{x1} - n\Delta k_{12}$  and  $k_{x2} + n\Delta k_{12}$  ( $n = 1, 2, \dots$ ,  $\Delta k_{12} = k_{x2} - k_{x1}$ ) are excited by FWM interactions of the newly generated FB modes with the modes that have excited them. This scenario goes on and on, and new FB modes are sequentially generated, until these modes reach the edge of the first BZ. The evolution from that point and on depends on the commensurability of  $\Delta k_{12}$  and the lattice momentum  $G$ .

If the momentum difference between the two initial FB modes,  $\Delta k_{12}$ , is commensurable with the width of the BZ (i.e.,  $\Delta k_{12} = \alpha G$  with a rational  $\alpha = m/l$ ,  $m$  and  $l$  being coprime integers), then the nonlinear interaction leads to the appearance of a comb of FB modes, consisting of only  $l$  modes in each band. For example, see Fig. 1, for which  $m = 1$ ,  $l = 5$ ,  $\alpha = 1/5$ . On the other hand, if  $\Delta k_{12}$  is incommensurable with  $G$ , the nonlinear interaction excites an infinitely dense set of modes (Fig. 2, for which  $\alpha \approx 1/8.6$  is irrational, to within a reasonable experimental accuracy). The explanation of both phenomena has to do with the fact that the lattice can contribute an integer

quantum of lattice momentum  $G$  to the nonlinear interaction. When a newly generated FB mode is close to the edge of the BZ and it interacts with another mode, subtracting (or adding) lattice momentum folds the interaction outcome back into the first BZ. In the commensurable case, this folding always falls onto an already excited FB mode, thus keeping the number of populated modes a finite discrete set (a comb). On the other hand, in the incommensurable case [Fig. 2], folding maps onto new modes, until eventually all FB modes of a particular band are populated [24]. This is the case of SC generation or equipartition: redistribution of energy between the linear modes of a periodic system as a result of nonlinearity.

Experimentally, we investigate the formation of spatial supercontinuum and frequency combs in a 1D nonlinear lattice fabricated in lithium niobate ( $\text{LiNbO}_3$ ). Our 1D waveguide array is fabricated by in-diffusion of Ti on a Fe-doped  $\text{LiNbO}_3$  wafer, exhibiting a photovoltaic self-defocusing nonlinearity. The array consists of approximately 250 stripes with a width of  $6 \mu\text{m}$  and a grating period  $\Lambda = 10 \mu\text{m}$ , and the ferroelectric axis points along the  $x$  direction. The band spectrum consists of three guided bands, which are separated by gaps. The experimental setup for the generation of spatial supercontinuum and frequency combs is sketched in Fig. 3. We use a continuous wave  $\lambda = 532 \text{ nm}$  laser beam (Verdi V2), polarized extraordinarily to utilize the largest electro-optic coefficient  $r_{33}$  of the  $\text{LiNbO}_3$  crystal. The beam is first expanded to a diameter of 30 mm (“plane wave”). Using an aperture of 2 mm diameter, we select the central part (having a constant intensity) to excite  $\sim 200$  channels of the array. To excite the proper FB modes, the wave is split into two beams of equal power, which are subsequently recombined at a controllable angle. We then use a prism pair (made of high-index Rutile) to couple the two beams simultaneously into, and out of, the waveguide array. Making use of the prism coupling method [25], we selectively excite any desired FB mode (or combinations of several modes) in the array by proper adjustment of the incidence angle. The intensity of the light leaving the in-coupling prism is measured by a photodiode (PD), which allows for exact adjustment of the transverse phase matching condition for excitation of a particular FB mode [26]. The light coupled out by the second prism is recorded by a CCD camera,

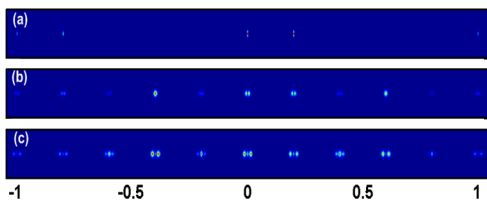


FIG. 1 (color online). Calculated evolution of the field Fourier power spectrum when two modes are launched into the array with QM difference  $\Delta k_{12} = G/5$  (commensurate case). Input beam (a), and after 3 mm (b) and 6 mm (c) of propagation. Here the distance of 6 mm is related to the experimental situation.

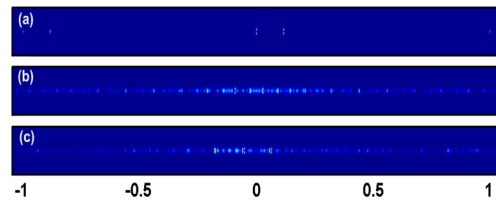


FIG. 2 (color online). Calculated evolution of the field Fourier power spectrum when two modes are launched into the array with QM difference  $\Delta k_{12} \approx G/8.6$  (incommensurate case). Input beam (a), and after 3 mm (b), and 6 mm (c) of propagation.

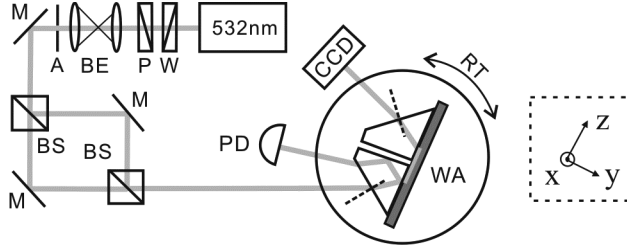


FIG. 3. Schematic experimental setup. W,  $\lambda/2$  plate; P, polarizer; BE, beam expander; A, aperture; M's, mirrors; BS's, beam splitters; PD, photodiode; CCD, CCD camera; WA, waveguide array; RT, rotary stage.

which directly yields the Fourier power spectrum inside the array.

In our experiment, we adjust the two input beams to excite simultaneously two different FB modes of the first band, having different wave vectors  $k_1$  and  $k_2$ , with  $k_2 - k_1 \approx k_{x2} - k_{x1} = \Delta k_{12}$  [see Fig. 4(a)]. The angles between the directions of the input beams and the propagation direction ( $z$  direction) in the array determine the transverse wave vectors, thereby determining the Bloch momenta of the excited modes. As such, we can readily adjust the Bloch momentum difference of the excited modes by superimposing the two input beams at the prism base with a small angle difference in the  $xz$  plane. In all measurements, one beam (marked as B2) is launched to excite a mode with Bloch momentum  $k_{x2} = 0$ . The other beam (marked as B1) is adjusted to excite a mode with a QM difference  $\Delta k_{12}$  relative to  $k_{x2}$ . Here  $\Delta k_{12}$  can be chosen to

be either incommensurable or commensurable with the width  $G$  of the BZ.

In the first experiment, we investigate the formation of a comb of spatial frequencies. For this commensurate case, the momentum difference is adjusted to  $\Delta k_{12} = G/5$ . In Fig. 4, we image the output Fourier spectra in two full BZ's, to provide a better perspective of the fashion in which evenly-spaced FB modes are sequentially excited, and overlap at the border between two neighboring BZ's. Figure 4(b) depicts the output Fourier spectra, under linear conditions, when B1 and B2 are excited, either simultaneously or individually. Here the propagation distance is 6 mm and the input optical power is rather low (25 nW per channel), thus avoiding any build-up of nonlinear index changes in the array. As clearly shown in Fig. 4(c), when the optical input power is increased to  $0.9 \mu\text{W}$  per channel, the increasing nonlinearity triggers the formation of a comb of spatial frequencies. Beginning with the two initially excited modes, the spectrum eventually develops into a comb containing 5 FB modes in the first BZ, in agreement with the theory about the anticipated number of modes in each band [23].

Next, we change the setup to observe spatial SC formation. For this the angle between the two input waves is now chosen to be incommensurable with the lattice momentum; here the relation between those is approximately  $\Delta k_{12} = G/8.24$  [see Fig. 5(a)]. All other parameters (propagation length, input powers) are the same as before. In Fig. 5(b) the linear Fourier spectra of excited modes are given. Again, we do not observe any energy exchange between the two FB modes under such linear conditions. However, for increased input power, the system becomes highly nonlinear, giving rise to coupling between FB modes and to energy spreading. This result is obvious in Fig. 5(c), which depicts the output power spectrum as the nonlinear interaction builds up in time, becoming stronger and stronger. After switching on the input light at time  $t = 0$ , a cascaded excitation of FB modes starts, which, at the beginning, is dominated by appearance of additional side bands separated by QM  $\pm \Delta k_{12}$  relative to  $k_{x1}$  and  $k_{x2}$ . With increasing time, also (initially weak) scattered waves start to increase in power and interact via FWM with other FB modes. Finally, after  $t = 20$  minutes (this rather large time constant is related to the low mobility of our samples: low charge mobility yields large photovoltaic fields, hence all efficient photovoltaic materials have low mobility), a broad spectrum of FB modes covering almost the full BZ has developed.

The results presented in Figs. 4 and 5 nicely agree with the main predictions outlined in [23]. However, our experiments also reveal new interesting additional effects. Observing Fig. 4 carefully reveals that most of the Fourier components in the comb exhibit a double-peak structure: almost every intensity peak in Fourier space is split in two. Studying this phenomenon numerically (for example by varying the number of excited channels, i.e., changing the width of the super-Gaussian beam we use as

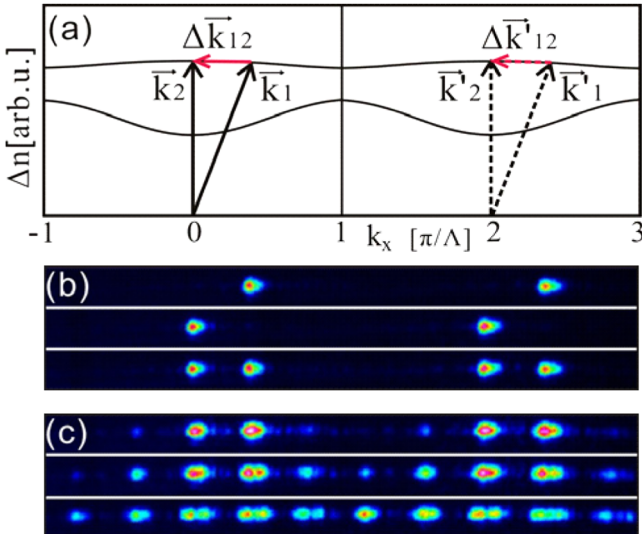


FIG. 4 (color online). Formation of spatial FC in the commensurate case with  $\Delta k_{12} = G/5$ . (a) Schematic band structure and excited modes. Here  $\Delta n = n_{\text{eff}} - n_{\text{sub}}$  represents the effective refractive index of the FB modes; (b) output linear Fourier spectra when B1 (top), B2 (middle), and both B1 and B2 (bottom) are excited; (c) nonlinear evolution of Fourier output spectra after  $t = 0.5$ , 1.5, and 5 min (from top to bottom).

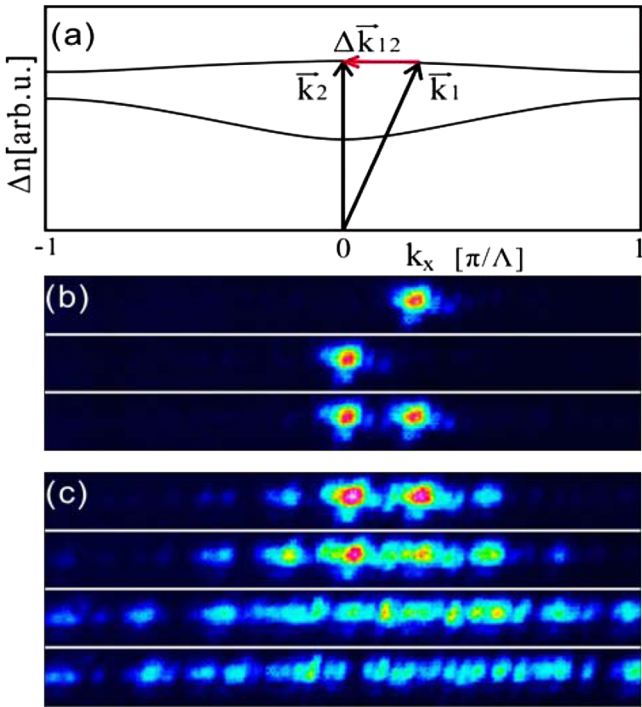


FIG. 5 (color online). Generation of SC in the incommensurate case with  $\Delta k_{12} \approx G/8.24$ . (a) Schematic band structure and the two FB modes; (b) output linear Fourier spectra when B1 (top), B2 (middle), and both B1 and B2 (bottom) are excited; (c) nonlinear evolution of Fourier output spectra. Photographs (from top to bottom) are taken after  $t = 0.5, 1.5, 5$ , and 20 min, respectively.

the launch beam) shows that the double-peak effect results from the fact that any finite beam has finite width in Fourier space, and the plane waves comprising each Fourier-peak interact with another through FWM. This phenomenon occurs also in a homogenous system (and is related to holographic scattering [27]). However, in a periodic structure the dispersion inside the band is weaker, and hence the phase matching is better; thus, the resulting peak-splitting is more apparent. In addition, we find that, if, in the simulation, a weak additional wave (of the same wavelength as B1 and B2, but with optical power of only  $\sim 1\%$  of them) is launched together with the two input waves into the lattice, this weak wave considerably accelerates the frequency comb or SC generation processes, although naturally it has no apparent effect on the (very dense, almost continuous) spectrum. In the experiment [see, e.g., Fig. 5(b)], although we illuminate our sample only by two plane waves, we always observe such very weak scattered waves adjacent to the two fundamental FB modes. The origin of these waves is attributed to multiple reflections in the Mach-Zehnder interferometer and the coupling prism, or, in the nonlinear case, additional waves formed by holographic scattering inside the array [27].

In summary, we have demonstrated experimentally the generation of spatial FC and of spatial SC resulting from

cascaded FWM interactions in 1D photonic lattices. These phenomena display a sensitive dependence on the difference of the FB momentum between the two initially-excited modes and the lattice momentum. We find that an additional weak wave accelerates both processes. We emphasize that both phenomena are universal, and apply to all nonlinear periodic structures in which waves propagate. In this vein, both SC and FC generation should be observable in Bose-Einstein condensates (BEC) in optical lattices, with both attractive and repulsive interactions.

We acknowledge financial support by the Deutsche Forschungsgemeinschaft (KI482/10-1), the German Federal Ministry of Education and Research (CHN 07/040), the Ministry of Science and Technology of P. R. China (2005DFA10170), GIF (grant 949-8.14/2007), and DIP (grant E6.1).

- [1] D. N. Christodoulides, F. Lederer, and Y. Silberberg, *Nature (London)* **424**, 817 (2003).
- [2] E. Fermi, J. Pasta, and S. Ulam, Los Alamos Report No. LA-1940 (1955).
- [3] J. Meier *et al.*, *Phys. Rev. Lett.* **92**, 163902 (2004).
- [4] D. Kip *et al.*, *Science* **290**, 495 (2000).
- [5] D. N. Christodoulides and R. I. Joseph, *Opt. Lett.* **13**, 794 (1988).
- [6] H. S. Eisenberg *et al.*, *Phys. Rev. Lett.* **81**, 3383 (1998).
- [7] J. W. Fleischer *et al.*, *Nature (London)* **422**, 147 (2003).
- [8] J. Meier *et al.*, *Phys. Rev. Lett.* **93**, 093903 (2004).
- [9] M. Stepić *et al.*, *Phys. Rev. E* **74**, 046614 (2006).
- [10] G. Bartal, O. Manela, and M. Segev, *Phys. Rev. Lett.* **97**, 073906 (2006).
- [11] R. Morandotti *et al.*, *Phys. Rev. Lett.* **86**, 3296 (2001).
- [12] H. S. Eisenberg *et al.*, *Phys. Rev. Lett.* **85**, 1863 (2000).
- [13] P. Millar *et al.*, *J. Opt. Soc. Am. B* **14**, 3224 (1997).
- [14] R. Iwanow *et al.*, *Opto-Electron. Rev.* **13**, 113 (2005).
- [15] J. W. Fleischer *et al.*, *Phys. Rev. Lett.* **90**, 023902 (2003).
- [16] F. Chen *et al.*, *Opt. Express* **13**, 4314 (2005).
- [17] A. Fratalocchi *et al.*, *Opt. Express* **13**, 1808 (2005).
- [18] J. K. Ranka, R. S. Windeler, and A. J. Stentz, *Opt. Lett.* **25**, 25 (2000).
- [19] J. Herrmann *et al.*, *Phys. Rev. Lett.* **88**, 173901 (2002).
- [20] A. V. Grobach and D. V. Skryabin, *Nat. Photon.* **1**, 653 (2007).
- [21] R. R. Alfano and S. L. Shapiro, *Phys. Rev. Lett.* **24**, 584 (1970).
- [22] J. M. Dudley, G. Genty, and S. Coen, *Rev. Mod. Phys.* **78**, 1135 (2006).
- [23] O. Manela *et al.*, *Opt. Lett.* **31**, 2320 (2006).
- [24] Adding lattice momentum can also lead to population of new bands, however the overlap integral—determining the coupling efficiency—between FB modes of different bands is not very large.
- [25] P. K. Tien and R. Ulrich, *J. Opt. Soc. Am.* **60**, 1325 (1970).
- [26] C. E. Rüter, J. Wisniewski, and D. Kip, *Opt. Lett.* **31**, 2768 (2006).
- [27] R. A. Rupp and F. W. Drees, *Appl. Phys. B* **39**, 223 (1986).